Available online at www.sciencedirect.com

ScienceDirect

Journal of the European Ceramic Society 27 (2007) 831–836

www.elsevier.com/locate/jeurceramsoc

The preparation and structural characterization of Al_2O_3/Ni–P composites with an interpenetrating network

J. Michalski[a,*], T. Wejrzanowski[a], S. Gierlotka[c], J. Bielinski[b], K. Konopka[a], T. Kosmac[d], K.J. Kurzydlowski[a]

[a] Faculty of Materials Science & Engineering, Warsaw University of Technology, Woloska 141, 02-507 Warsaw, Poland
[b] Faculty of Chemistry, Warsaw University of Technology, Noakowskiego 3, 00-664 Warsaw, Poland
[c] High Pressure Research Center of Polish Academy of Science, Sokolowska 29, 01-142 Warsaw, Poland
[d] Josef Stefan Institute, Jamova 39, 1001 Ljubljana, Slovenia

Available online 6 October 2006

Abstract

This paper reports on the possibility of obtaining 3D interpenetrating ceramic–metal composites by using an electroless chemical plating method. Alumina powder was coated with a homogenous Ni–P alloy layer to obtain Al_2O_3/Ni–P composites. The coated powders were consolidated via hot pressing (HP) under high pressure at different temperatures below the melting point of the metal phase. High-resolution scanning electron microscope (HRSEM) and X-ray diffractometry (XRD) techniques were used to study the influence of the consolidation conditions (temperature and pressure) on the microstructure of the composites. The percolation of the interpenetrating phases was evaluated by computer-aided image analysis and electrical conductivity measurements. The results indicate that the use of electroless nickel plating allows for the fabrication of uniform 3D interpenetrating, continuous metal–ceramic composites. The metal phase fills the open pores and also interpenetrates the spaces between the ceramic grains. Depending on the consolidation conditions it is possible to obtain dense or porous materials with a promising metal phase nanostructure.

© 2006 Elsevier Ltd. All rights reserved.

Keywords: Al_2O_3; Powders-chemical preparation; Nanocomposites; Hot pressing; Interpenetrating structure

1. Introduction

Ceramic particles have been added to metals since the 1930s in order to improve their mechanical properties. Additions of ceramics to light metals, like aluminium and magnesium, is designed to produce metal–matrix composites with higher strength, stiffness, hardness, wear resistance and reduce the coefficient of thermal expansion. At the same time, ceramic–matrix composites with metal particles have been developed to improve the mechanical and functional properties of ceramic materials, properties like brittleness, toughness, ferromagnetism and dielectric constant. In both cases the one of the phases appears in the form of particles and the other forms the matrix. The properties of these composites depend to a large degree on the properties of the matrix, and the influence of the dispersed phase is limited partly by proportionality to its volume fraction. For this reason, during the past 10 years there has been rapid progress in developing a new kind of composites interconnected phases. This new class of composites is called the interpenetrating phase composite. The microstructure of these materials is characterized by continuity of two or more phases, and the materials exhibit multifunctional macroscopic properties directly as a result of the specific properties of each phase.

The processing and properties of ceramic–metal composites with an interpenetrating microstructure have been reported in a number of papers.[1–4] The frequently used processing technologies for such composites include: pressureless or pressure-assisted molten-metal infiltration of a porous ceramic preforms,[5] reactive metal infiltration[6] and the displacement reaction. Powder metallurgy has proved to be less efficient in this context as frequently results in discontinuous or partially discontinuous distribution of phases.

In the present study an alternative method of fabricating ceramic–metal composites with an interpenetrating network based on electroless nickel plating and a powder-metallurgy technique is proposed. The Al_2O_3/Ni–P composites were pro-

---

[*] Corresponding author. Tel.: +48 22 660 87 40; fax: +48 22 660 87 50.
E-mail address: jmichalski@inmat.pw.edu.pl (J. Michalski).

0955-2219/$ – see front matter © 2006 Elsevier Ltd. All rights reserved.
doi:10.1016/j.jeurceramsoc.2006.04.034

duced by high-pressure (7 GPa) hot pressing of alumina powders that were homogenously coated with a thin nanometric layer of Ni–P alloy in an autocatalytic chemical process. The microstructures of composites obtained in such a way were analysed in terms of the continuity of the metal and alumina. For this purpose, electrical conductivity measurements, computer image analyses and XRD were used. Simultaneously, the influence of the high pressure at different sintering temperatures on the morphology, phase structure and electrical conductivity were investigated.

2. Experimental

In this investigation α-alumina powder CT800SG (Alcoa Industrial Chemicals) with an average grain size of 2.5 μm and a purity of 99.5% was used. The powder was initially ball milled in a planetary mill for 1 h in isopropanol to break up the agglomerates, then dried and sieved. The surface of the powder was sensitized in a $SnCl_2{\cdot}2H_2O$ bath, centrifuged, washed in water and again centrifuged. In the next step the sensitized powder was activated in a $PdCl_2{\cdot}2H_2O$ bath, centrifuged and washed in water. The zeta-potential was measured (with a ZeataPALS zeta-potential analyser from Brookhaven Instruments Co.) after each step of the process and also after the initial milling. The particle size distribution was measured with a Cials 850 granulometer after the same processes.

The powder was plated with a Ni–P alloy in an electroless nickel plating bath. The composition of the nickel plating bath is listed in Table 1. The temperature of the nickel plating bath was maintained at 60–70 °C and the pH at 9.

After drying, the plated powder was sintered at four temperatures (room temperature, 600, 800 and 1000 °C), via a hot-pressing method under a pressure of 7 GPa, in a special toroidal die made from lithographic stone (calcium carbonate).[7] The samples were fabricated in the form of cylinders 5 mm in diameter and 5 mm high. The morphology of the coating and the composite microstructure after the consolidation were examined with a high-resolution scanning electron microscope (HRSEM) with a thermally assisted Schottky field emitter. Samples for the microstructure observations were prepared via a mechanical grinding and ion-milling technique. The amount of deposited Ni–P alloy and the content of phosphorus were measured by a chemical method based on the spectral-photometric method with the use of molibdate blue. The theoretical density was calculated by using the mixture law and the bulk densities of the consolidated samples were measured using the Archimedes method with de-ionized water as the liquid medium. The phase structure of the composite and the grain size of the metal phase were investigated using X-ray diffractometry (XRD) with Cu Kα radiation.

Table 1
The composition of the sensitizing, activating and electroless nickel plating baths

Reagent	Concentration
Sensitization	
$SnCl_2{\cdot}2H_2O$	10 g/L
Activation	
$PdCl_2{\cdot}2H_2O$	1 g/L
Electroless nickel plating	
$NiSO_4$	0.1 mol/L
NaH_2PO_4	0.2 mol/L
NH_2CH_2COOH	0.2 mol/L
Buffer agents	

The microstructure of the obtained materials were quantitatively analysed using image analysis methods. A computer program was developed for analyses of the continuity of Al_2O_3 and Ni–P. At least 10^6 randomly oriented and positioned lines were used in order to achieve sufficiently good statistics. Images for analyses have been randomly selected from the surface of studied specimens. Two quantitative parameters, proposed by Gurland,[8] were used to characterize the studied material structure. One is the continuity, C, and the second the percolation factor, P_r. Continuity was defined as the fraction of the internal surface of the α phase shared with the other α phase particles in the α/β two-phase mixture. The continuity varies between 0 and 1 as the continuity path of one phase in the other changes from a completely dispersed to a fully agglomerated structure. The percolation factor quantifies features opposite to continuity, and determinates whether the α phase is fully surrounded by the β phase (then $P_r = 1$) or the β phase is spread among the α phase (then P_r is close to 0).

The continuity and percolation factors can be expressed by the following equations:

$$P_r = 1 - C_\alpha, \tag{1}$$

$$C_\alpha = \frac{2N_L^{\alpha\alpha}}{2N_L^{\alpha\alpha} + N_L^{\alpha\beta}}. \tag{2}$$

where P_r is the percolation of the α phase by the β phase, C_α the continuity of the α phase, $N_L^{\alpha\alpha}$and $N_L^{\alpha\beta}$ are the numbers of α/α and α/β intercepts per unit length. The percolation and the continuity factors for the Al_2O_3 phase were calculated using Eqs. (1) and (2).

In order to fully characterize the interpenetrating character of the composite microstructures, in particular the continuity of the metal phase, the conductivity of samples was measured using an ac current (frequency 100 Hz) with an LCR meter (Agilent 4284A). The resistivity was calculated using Eq. (3):

$$\rho_e = \frac{RA}{l} \tag{3}$$

where R is the measured resistance, A the area of the samples and l is the length of the samples between the electrodes.

3. Results

3.1. Powder preparation

Measurements of the zeta-potential of the powder after each stage of powder preparation before nickel plating made it possible to optimize the pH of the sensitization and activation baths, which then helped to prevent re-agglomeration. Fig. 1 shows that the powder is in a stable state when the bath pH is lower

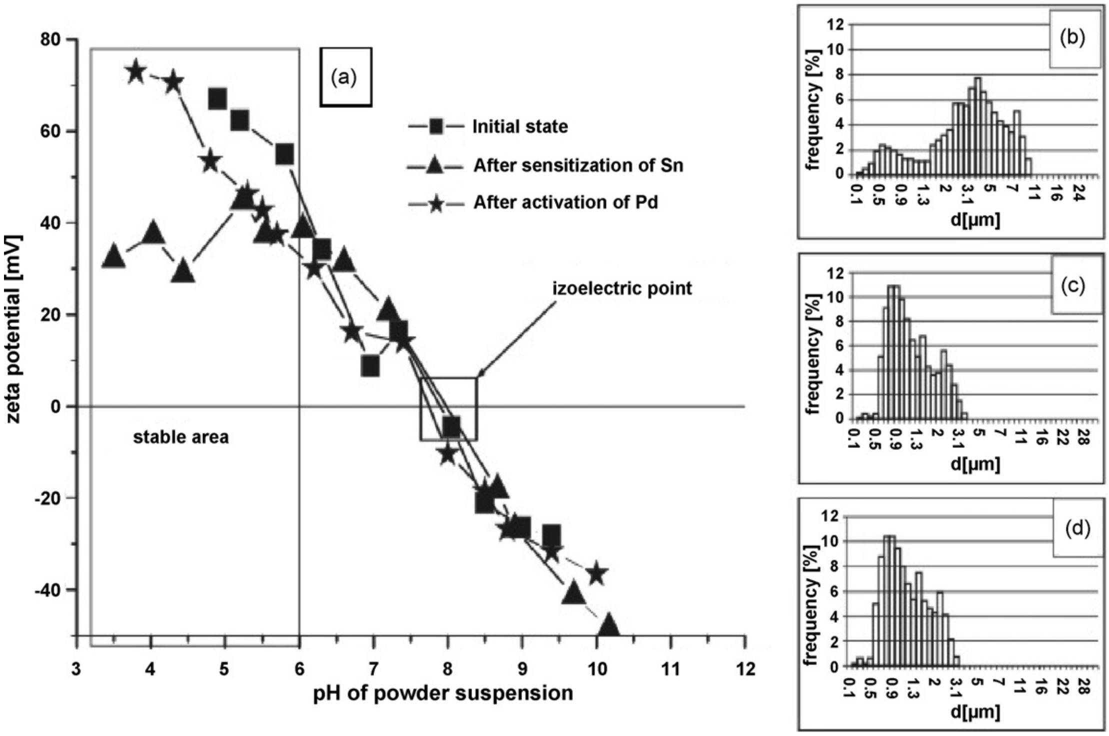

Fig. 1. The zeta-potential vs. pH measured for the powder in the initial state and after the sensitization and activation processes (a) and particles size distributions of the powder: in initial state (b), after sensitization (c) and after activation (d).

than 6, as confirmed by the particle size distributions measured for the powder in the initial state and after the sensitization and activation processes. (The same position of the iso-electric point measured for the powder in the initial state and after the sensitization and activation processes is most likely a coincidence.)

After nickel plating the colour of the alumina powder changed from white to black. SEM investigations in back-scattered electrons (BSE), which make possible to observe the contrast from associated with the average *Z* number, showed that the surfaces of the alumina grains were uniformly coated with a thin layer of Ni–P alloy (Fig. 2a). The layer was made up of nano-aggregates of particles having a size close to 10 nm, as observed using HRSEM in the secondary-electrons (SE) mode. The results of the chemical analyses revealed that the coated powder consisted of ∼28 wt.% of Ni–P, which contained ∼2 wt.% of P.

3.2. Composite density

The theoretical density of the composites was calculated using the rule of mixture and the following density values: the ratio of metal to alumina, 28:72 (w/w); the density of alumina, 3.98 g/cm^3; the density of Ni–P alloy, 8.3 g/cm^3. This value is equal to 4.66 g/cm^3. The bulk density of the composites measured by the Archimedes method revealed that the density of the samples after pressing at room temperature reached 82% of the theoretical density. Density of the samples pressed at 600, 800 and 1000 °C is listed in Table 2.

3.3. Microstructure and phase analyses

The XRD patterns of the Ni–P-coated alumina powder and the composites after pressing under a pressure of 7 GPa at room

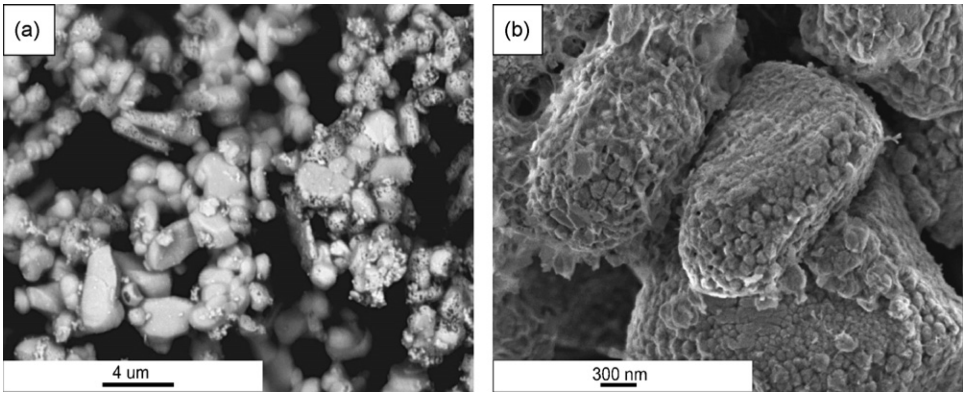

Fig. 2. SEM pictures of the powder electroless plated with the Ni–P alloy: (a) in BSE mode and (b) in SE mode.

Table 2
Results of the microstructure analyses, the resistivity measurements and the grain size of the Ni–P calculated from the XRD patterns

Consolidation temperature	Percolation factor, P_r (%)	Continuity of alumina, C_α	Resistivity, ρ_e ($10^{-2}\ \Omega$ cm)	Ni–P grain size (nm)	Bulk density (g/cm^3)
Room temperature	84	0.16	42	10	3.81
600 °C	73	0.27	8.7	26	4.63
800 °C	69	0.31	2	74	4.22
1000 °C	47	0.53	8.7	76	4.36

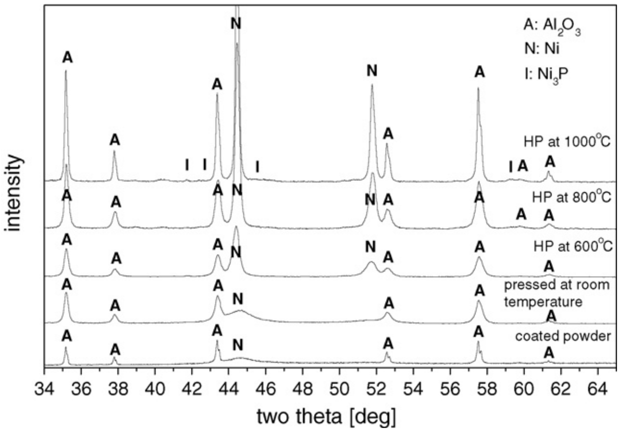

Fig. 3. Diffraction patterns for as-coated powder, and composites after pressing at room temperature and at 600, 800 and 1000 °C.

temperature, 600, 800 and 1000 °C are shown in Fig. 3. In the case of the composite powder and the sample after pressing at room temperature only one peak from Ni is visible. The broadened shape of this peak indicates the nanometric character of the metal phase after the deposition and after the pressing process. This nano-size of the metal grains was confirmed by a calculation with the Williamson–Hall method using[9] the results given in Table 2. In addition, the nanometric character is also visible on the HRSEM pictures of the coated powder (Fig. 2b) and the ion-etched cross-section of the composite after pressing at room temperature (Fig. 4a). The increase of the pressing temperature results in a sharpening of the Ni peaks. However, the width of the peaks from all of the samples points to a nanometric grain size for the metal phase. The results of the calculation show that the grain size increases from room temperature up to 800 °C and then stabilizes for temperatures between 800 and 1000 °C, remaining lower than 100 nm, Table 2. No nickel oxide peaks were detected in the XRD patterns of the samples. Small peaks of the Ni_3P phase were only observed in the XRD pattern from the samples pressed at 1000 °C.

HRSEM observations of the microstructures (Fig. 4) confirm the isotropic and percolated character of the obtained composites. This has been corroborated by the computer image analyses. The percolation factor of this structure changes with the hot-pressing temperature. The parameter P_r decreases as the sin-

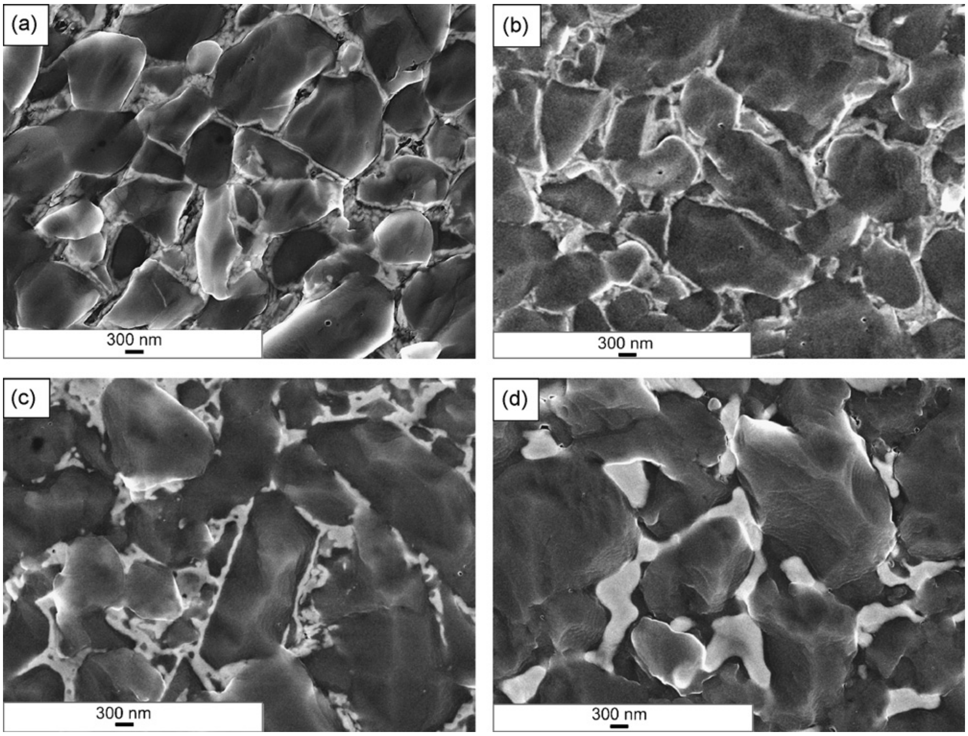

Fig. 4. HRSEM pictures of the ion-etched surfaces of the composites: (a) after pressing at room temperature, and after hot pressing at (b) 600 °C, (c) 800 °C and (d) 1000 °C.

tering temperature increases. Simultaneously, the continuity of the alumina phase increases (see Table 2). All of the investigated samples were conductive, which means that the continuity of Ni grains was also maintained across the whole range of temperatures.

4. Discussion

The possibility of obtaining homogenous, low-phosphorus, electroless-deposited Ni–P layers on the surface of alumina powder was studied with respect to the effects of the processing parameters. The results of the zeta-potential measurements (Fig. 1a) revealed the need to apply the sensitizing and activation baths, the pH of which should be lower than 6. In this range of pH the powder stays in the stable area of high zeta-potentials. The measured values of the zeta-potential lay above 40 mV, which indicates that the charge on the surface of each particle have the same positive sign preventing agglomeration during the processes. This makes it possible to obtain a more homogeneous dispersion of the Pd(0) active centres before the nickel plating process. On the graph a slight decrease of the measured zeta-potential for a pH below 5 for the powder after sensitization can be found. However, it seems not to have any influence on the powder agglomeration, as indicated by the results of the particle size measurements (Fig. 1b–d). Furthermore, during the first step of the electroless nickel plating process, when the Ni–P is deposited on the palladium active centres, the homogenous distributions of Pd(0) allowed a uniform plating of the powder with a Ni–P layer, as indicated by the images shown in Fig. 2b obtained using the BSE detector.

The structure of the electroless-deposited Ni–P layers is determined by the phosphorus content. Generally, the layers with low phosphorus content have a nanocrystalline structure, which changes to an amorphous structure with an increasing P concentration.[10] Earlier investigations showed that the amount of P in the Ni–P layers strongly depends on the pH of the electroless plating bath and decreases together with an increase in the pH.[11] For example, changing the pH of the baths from 4 to 8 resulted in a decrease in the amount of phosphorus from 11 to 3 wt.% in the deposited layers. Simultaneously with a change in the pH to alkaline a considerable increase in the deposition rate was observed. In the present investigation the pH of the electroless nickel plating bath was ∼9, which resulted in a small amount of P in the deposited material (∼2 wt.%), its nanocrystalline character (grain size ∼ 10 nm), and the high speed of the reaction, which then makes it possible to have a uniform coating in a short process time (5 min).

At atmospheric pressure the melting point of a nickel–2% phosphorus alloy is 870 °C. As the results show, during the pressureless sintering of the composite, the melting temperature is higher and the metal layers melt and are de-wetted from the alumina surface forming spherical particles dispersed in the alumina matrix.[12] Literature data[13] show that high pressures increase the melting temperature of the Ni. This has been confirmed with regard to the Ni–P alloy by sintering at 7 GPa, which shifted the melting point from 870 to ∼1100 °C.[14] In this way, high pressure sintering has led to the formation of a continuous Ni–P phase in the composite microstructure. Such structure has been observed in samples obtained by pressing at room temperature (Fig. 4a) and at 600, 800 and 1000 °C (Fig. 4b–d). The continuity of the metal phases was confirmed by the results of the conductivity measurements. However, the level of continuity of the structure was variable. The increase of the temperature during the HP process resulted in the percolation factor, P_r, decreasing, Table 2, which means that the metal phase was becoming less continuous. This lowest continuity of the metal phase is a result of the plastic deformation of the Ni–P alloy and its extrusion from between the alumina grains. The “squeezed” metal fills out the open pores (independent of their size and shape). Simultaneously, with the increase of the temperature the Ni–P particles start to sinter together, which results in their growth (see Table 2). These two phenomena result in the density increase from 82% of the theoretical density for the samples after pressing at room temperature to nearly 100% of the theoretical density for the samples after the HP process.

The observed variations in the conductivity can be explained by the connection between the Ni–P nanoparticles in the samples after pressing at room temperature and after hot pressing. The observed changes are associated with the variation in the percolation of the phases and the differences in the magnitude of the cross-sections of the conductive paths. The sample after pressing at room temperature, which has the highest percolation factor but the poorest connection between the Ni–P particles and the small cross-sections of the conductive paths, exhibits the lowest conductivity. The highest conductivity was measured for the sample pressed at 800 °C, where the percolation factor was still relatively high, the metal phase was sintered and the cross-sections of the conductive paths were close to the 74 nm of the measured grain size.

Nickel–phosphorus binary phase diagram [15] shows that Ni_3P is the stable phase of the low-phosphorus nickel alloy at room temperature, and this phase is found in the XRD pattern after annealing at temperatures higher than 300 °C. In the present investigation the phosphide phases were detected during hot pressing at temperatures lower than 1000 °C. We suppose that this is the effect of applying the high pressure and is connected with the influence of the pressure on the melting temperature of the Ni–P alloy.

5. Conclusions

1. Electroless nickel plating can be used for fabrication Al_2O_3/Ni–P composite powder. The surface of each grain of powder is coated with a homogenous layer built with spherical nano-aggregates of Ni–P alloy. The morphology and chemical composition of the deposited materials can be controlled with the parameters of the plating process.
2. High pressure consolidation of the composite powders makes it possible to fabricate dense ceramic metal nanocomposites with a uniform, 3D interpenetrating structure. The continuity of this structure and the morphology of the metal phase strongly depend on the pressure and the sintering temperature.

3. The applied pressure increases the melting point of the Ni–P alloy and has an influence on its phase composition.

Acknowledgment

This research has been financially supported by the Polish State Committee for Scientific Research (project no. Nr 4T08D03225).

References

1. Mattern, A., Huchler, B., Staudenecker, D., Oberacker, R., Nagel, A. and Hoffmann, M. J., Preparation of interpenetrating ceramic–metal composites. *J. Eur. Ceram. Soc.*, 2004, **24**, 3399–3408.
2. Leverkoehne, M., Murthy, V. S. R., Janssen, R. and Claussen, N., Electrical resistivity of Cr–Al_2O_3 and Zr_xAl_y–Al_2O_3 composites with interpenetrating microstructure. *J. Eur. Ceram. Soc.*, 2002, **22**, 2149–2153.
3. Fahrenholtz, W. G., Ellerby, D. T. and Loehman, E. L., Al_2O_3–Ni composites with high strength end fracture toughness. *J. Am. Ceram. Soc.*, 2000, **83**(5), 1279–1280.
4. San Marchi, C., Kouzeli, M., Rao, R., Lewis, J. A. and Dunand, D. C., Alumina aluminium interpenetrating phase composites with three-dimensional periodic architecture. *Scripta Mater.*, 2003, **49**, 861–866.
5. Travitzky, N. A., Microstructure and mechanical properties of alumina/copper composites fabricated by different infiltration techniques. *Mater. Lett.*, 1998, **36**, 114–117.
6. Yoshikawa, N., Watanabe, Y., Matamoros Velloza, Z. M., Taniguchi, S. and Kikuchi, A., Mechanical properties of Al/Al_2O_3 composites fabricated by reaction between SiO_2 and molten Al, Al–Cu. *J. Mater. Sci. Lett.*, 1997, **16**, 1547–1550.
7. Gierlotka, S., Palosz, B. F., Swiderska-Sroda, A., Grzanka, E., Kalisz, G., Pietkiewicz, K. *et al.*, Synthesis of metal–ceramic nanocomposites by high pressure infiltration. *Solid State Phenom.*, 2005, **101–102**, 157–164.
8. Gurland, J., The measurement of grain continuity in two phases alloys. *Trans. Met. Soc. AIME*, 1958, **212**, 452–455.
9. Ungar, T., Dragomir-Cernatescu, I., Louer, D. and Andebrand, N., Dislocations and crystallite size distribution in nanocrystaline CeO_2 obtained an ammonium cerium(IV)-nitride solution. *J. Phys. Chem. Solids*, 2001, **62**, 1935–1941.
10. Faber, B., Cadel, E., Menand, A., Schmitz, G. and Kirchheim, R., Phosphorus segregation in nanocrystaline Ni–3.6 at% P alloy investigated with the tomographic atom probe. *Acta Mater.*, 2000, **48**, 789–796.
11. Bielinski, J., Kulak, I., Bielinska, A. and Michalski, J., Bezprądowe niklowanie materiałów litych i proszkowych. *Ochrona przed korozją*, 2003, **46**(11A), 233–237.
12. Michalski, J., Konopka, K. and Trzaska, M., Description of Al_2O_3 powders coated by Ni–P particles obtained through an electroless chemical reaction and possibilities to obtain an Al_2O_3/Ni–P composite. *Mater. Chem. Phys.*, 2003, **81**, 407–410.
13. Cannon, J. F., Behavior of the elements at high pressures. *Phys. Chem. Ref. data*, 1974, **3**(3), 781–824.
14. Michalski, J., Konopka, K., Gierlotka, S. and Kurzydlowski, K. J., Influence of temperature and pressure on the possibility of obtaining Al_2O_3/Ni–P nanocomposites through hot pressing process. *Solid State Phenom.*, 2005, **101–102**, 147–150.
15. Massalski, T. B., Okamoto, H., Subramanian, P. R. and Kacprzyk, L., (*2nd ed.*). *Binary Alloy Phase Diagrams*, *Vol. 3*SAM International, Materials Park, OH, 1992.